

MICROSTRUCTURE AND CORROSION BEHAVIOUR OF AUSTENITIC STAINLESS STEEL TREATED WITH LASER

Ibrahim Y.A. Khalfallah, Mohammed N. Rahoma*, and Jaafar H. Abboud

Department of Mechanical Engineering, Faculty of Engineering,
Garyounis University, Benghazi, Libya, P.O.Box 1308
E mail: younis_ibrahem@yahoo.com, E mail: jhabooud@yahoo.com

* Department of Chemistry, Science College,
Garyounis University, Benghazi, Libya, P.O. Box 1308
E mail: Rahuma@garyounis.edu

الملخص

تم دراسة تأثير المعالجة السطحية باستخدام الاشعة المنبعثة من ليزر ثاني اكسيد الكربون المستمر بقدرة 2 و 4 كيلو واط وسرع مختلفة تراوحت ما بين 300 إلى 1500 ملم بالدقيقة على خواص الفولاذ الاوستنايتي المقاوم للتآكل 316. كما تم دراسة السطحي مع الكربون لنفس الفولاذ بالليزر وذلك بطلاء الفولاذ بمسحوق الجرافيت قبل الصهر بالليزر بهدف تصليد المعدن من غير ان تتأثر باقي اجزاء المعدن. استخدمت عدة تقنيات ميتالورجية لدراسة البنية المجهرية بعد وقبل المعالجة بالليزر مثل المجهر الضوئي والمجهر الالكتروني الماسح و حيود الأشعة السينية وجهاز قياس الصلادة الدقيق. لدراسة مقاومة التآكل للعينات المعالجة بالليزر ومقارنتها بالمعدن الاساسي باستخدام جهاز قياسات الجهد الكهروكيميائية. بينت النتائج ان الصهر بالليزر ادى الى الحصول بنية شجيرية اوستنايتية ناعمة ومتجانسة مع زيادة طفيفة في الصلادة 200 إلى 230Hv بينما العينات المطلية بالكربون ادى الصهر بالليزر إلى تكوين بنية شجيرية اوستنايتية محاطة بشبكة من الكاربيدات مما نتج عنه زيادة كبيرة في الصلادة من 200Hv إلى 500Hv نتائج اختبار التآكل أوضحت بتحسّن ملحوظ لمقاومة التآكل وارتفاع قيمة الجهد بعد الصهر بالليزر مقارنة مع المعدن الاصلي بينما العينات التي سبكت مع الكربون انخفض فيها مقاومة التآكل. أوضحت النتائج بان تجانس البنية المجهرية بعد الصهر هو الذي ادى الى التحسّن الملحوظ في مقاومة التآكل بينما تكون الكريبيدات ادى الى انخفاض في مقاومة التآكل.

ABSTRACT

Surface modification of 316 stainless steel by laser melting was investigated experimentally using 2 and 4 kW continuous wave CO₂ laser and specimen scanning speeds ranged from 300 to 1500 mm/min. Also, an investigation is reported of the introduction of carbon into the same material by means of laser surface alloying which involved precoating the specimen surfaces with graphite powder followed by laser melting. The aim of these treatments is to enhance corrosion resistance by the rapid solidification associated with laser melting and also to increase surface hardness without affecting the bulk properties by increasing carbon concentration near the surface. Different metallurgical techniques such as optical microscopy, scanning electron microscopy (SEM), and X-ray diffraction (XRD) were used to characterize the microstructure of the treated zone. The microstructures of the laser melted zones exhibited a dendritic morphology with a very fine scale with a slight increase in hardness from 200 to 230 Hv. However, the laser alloyed samples with carbon showed

microstructure consisting γ dendrite surrounded by a network of eutectic structure ($\gamma +$ carbide). A significant increase in hardness from 200 to 500 Hv is obtained. Corrosion resistance was improved considerably after laser melting especially in the samples processed at high laser power (4kW). There was shift in the I_{corr} and E_{corr} toward more noble values and a lower passive current density than the untreated materials. These improvements in corrosion resistance were attributed due to the fine and homogeneous dendritic structure which was found throughout the melted zones. The corrosion resistance of the carburized sample was lower than the laser melted sample.

KEYWORDS: Laser; Austenitic stainless steel; Corrosion; Microstructure

INTRODUCTION

When a metallic surface is irradiated with a high power laser pulses, part of the energy is reflected and other is absorbed. The absorbed energy is “instantaneously” transferred to the lattice and rapidly raises the near-surface temperature and reaches the melting point. As a consequence to that, a liquid-solid interface starts to move downward into the metal. As soon as the laser pulse is finished the resolidification process begins from the liquid/solid interface towards the surface. Due to the high cooling rates (10^6 C/s), solid-state diffusion can be neglected and homogeneous and fine solidification microstructures can be achieved with a wide variety of surface compositions without the limitations of conventional processes, for instance, to extend solid solutions and to obtain metastable structures or even metallic glasses [1-4]. This technique has been widely used to treat the surfaces of different ferrous and nonferrous materials and considerable improvements in corrosion, erosion, and hardness has been reported due to the unique structure obtained after laser melting [5-6]. By coating the metal surface with some elements, usually in the form of powder, followed by laser melting; these alloying elements diffuse rapidly into the melt pool to a desired depth forming an alloyed layer in a short period of time. This technique is known as laser surface alloying (LSA) and by this technique; a desired alloy chemistry and microstructure can be generated on the sample surface. Various alloying elements in the form of metal powders suspended in liquid have been surface melted into AISI 1018 steel and electrodeposited chromium and plasma -sprayed molybdenum [7] have been surface melted into other steels. The concept of carburizing by laser melting was initially realized through the use of graphite coatings during laser surface hardening of steels, which served as an efficient way to increase the coupling of radiation with the steel substrate, which for the case of the CO_2 laser far-infrared radiation (wavelength 10.6m) is extremely low. It was then observed that substantial amount of carbon could be introduced to steel surfaces in that manner. Since then, studies have been reported on the laser carburizing of commercial pure iron [7], plain carbon [8], and low alloy steel [9].

Laser applications in the surface treatment of stainless steel have been focused on ferritic (AISI 430), martensitic (AISI 420) and austenitic (AISI 304 and AISI 310) types to improve pitting corrosion resistance [10]. In general, the corrosion resistance was improved after laser melting and It has been found that the corrosion resistance depends critically on the laser processing parameters, particularly for the cases of ferritic and martensitic [10-11]. The effect of laser melting of UNS S42000 steel on the cavitation erosion and pitting corrosion has been study in detail by Man and his co-workers [12]. It was found that cavitation erosion improved significantly after laser melting due to the

formation of large volume fraction of retained austenite which has high martensitic transformability.

The aim of the present work is to study the effect of laser surface melting and rapid solidification of austenitic 316 steel on the corrosion resistance and also to investigate the effect of laser surface alloying of the same material with carbon on the corrosion resistance and on the microhardness .

MATERIAL AND EXPERIMENTAL WORK

Material

The austenitic stainless steel used in the present work is AISI 316 supplied by the researches center of Tajoura. The material was rolled and annealed sheet of 5mm thickness. The chemical composition is given in Table (1) Several specimens of surface area 15mmx15mm were prepared by wire electrical discharge cutting machine. The sample surfaces were polished up to grade 800 to give a consistent surface finish. For laser surface alloying with carbon, a layer of graphite powder having particle size 5 μ m was mixed with a binder and applied as evenly as possible on the polished steel. The deposited graphite thickness was ~ 100 μ m. After graphite coating, the surfaces was ground with 800 grid emery paper to make the surface flat and uniform.

Table 1: Nominal chemical composition of the steels used in the study (wt. %)

Element	Fe	C	Cr	Ni	Mn	Si	Mo	P	S
Wt%	Bal.	0.08	16-18	10-14	2.0	1.0	3.0	0.045	0.03

The Laser

The laser machine used in this investigation is a CO₂ laser operating in a continuous and pulse mode. The maximum output power is 6 kW. The laser beam is focused by ZnSe lens with focal length 200 mm. The minimum diameter of the focused beam is about 0.47 mm. The relative movement between laser beam and work piece is realized by CNC (computer numerical control) X-Y-Z nozzle. For alignment procedures, a He Ne laser beam was transmitted along the optical axes. The distance between the laser beam focus point and the metal surface was kept about 10 mm; this gives a beam diameter of about 2 mm [13]

Laser surface melting and alloying

Laser surface melting was carried out using CW CO₂ laser of maximum power 6kW. Argon gas flowing at rate 900 l/hr was used as the shielding gas to prevent oxidation of the sample. Single and overlapping tracks were obtained by overlapping of successive melt tracks at 50% track width interval. Laser surface alloying was achieved by surface melting of the 316 steel which was coated with the graphite powder. Table (2) present the processing parameters used for LSM and LSA. More detail about the experimental work can be found in ref [13].

Table 2: Processing parameters used for LSM and LSA .

Specimen No.	Laser Power P(kW)	Scan Speed V (mm/min)	Specimen No.	Laser Power P (kW)	Scan Speed V (mm/min)
M-13#	2	300	A-19#	2	300
M-14#	2	900	A-20#	2	900
M-15#	2	1500	A-21#	2	1500
M-16#	4	300	A-22#	4	300
M-17#	4	900	A-23#	4	900
M-18#	4	1500	A-24#	4	1500

M: Melting, A: Alloying with carbon

Metallographic Examination

After laser treatments, cross sections were obtained by cutting the processed sample perpendicular to the beam direction, in order to allow for the observation below the surface of the materials. Microstructural study was performed by optical microscopy and scanning electron microscopy. Specimens were etched with a reagent consisting of (25 g FeCl₃, 25 ml HCl and 100 ml H₂O). X-ray diffraction was taken from the surface of the overlapped sample. Microhardness was measured as a function of depth below the surface for the entire laser treated specimen with a microhardness tester. The applied force is 200gf and 10sec.

Electrochemical Test

Potentiodynamic polarization scans were carried out using a Gill 12 stagnating the pitting corrosion behavior of laser surface modified and as-received specimens. 3.5% NaCl solution was kept at a constant temperature of 23°C and deaerated by purging with nitrogen for 1 h prior to corrosion tests. A saturated calomel electrode (SCE) was used as the reference electrode and auxiliary electrode was made of platinum. All data were recorded after an initial delay of one hour for the specimen to reach a steady state. (Figure 1).

RESULT AND DISCUSSION

Microstructure

Laser surface melting of 316 stainless steel at different laser powers and scanning speeds produce microstructure consisting of columnar grains grown epitaxially from the interface toward the top surface (Figure 2). Very fine dendrites were observed within these grains. The secondary arm spacing was estimated to be 2 to 3 μm suggested a very high cooling rate achieved during solidification. From the other side, the graphite coated sample showed a melted zone of bigger size compared to the uncoated 316 steel under the same processing conditions (Figure 3). This is due to the carbon which leads to improve the coupling efficiency between the laser beam and the substrate [7].

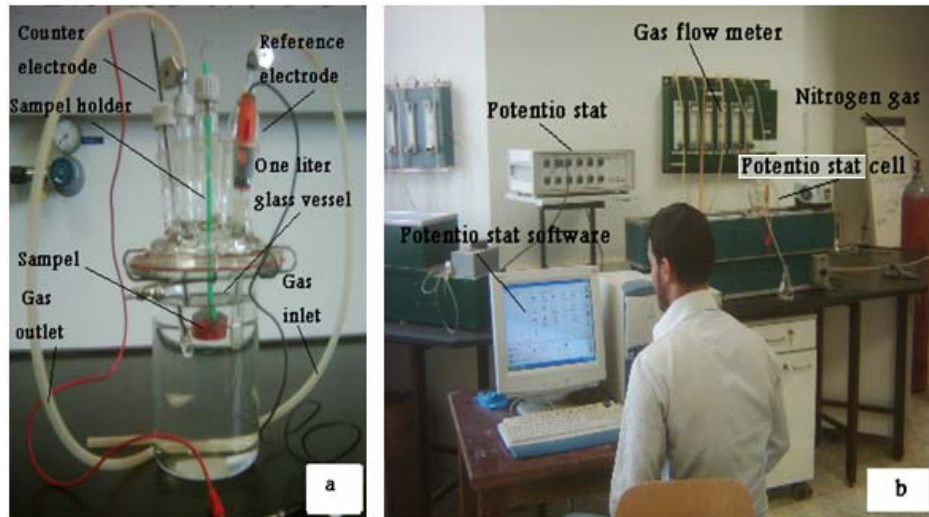


Figure 1: (a) Corrosion test cell (b) corrosion test system (Potentiostat test) .

It is evident from the micrographs in Figure (3) a and b that graphite powder dissolved completely in the molten pool and no evidence of free graphite was seen which indicates a good mixing and alloying between the graphite powder and the molten substrate. The alloyed zone display a fine dendritic structure homogeneously distributed in the melted zone (Figure 3a and b). The region adjacent to the interface showed a planar zone (appeared white) which becomes dendritic as the distance from the interface increased. This change in solidification mode from planar to dendritic can be interpreted on the basis of temperature gradient and growth rates. The temperature gradient and growth rate are important in the combined forms GR (cooling rate) and G/R since they influence the scale of the solidification substructure and solidification morphology, respectively. Examination of the structure at high magnification revealed a thin layer of a discontinuous carbide network located between the dendrites Figure (3b); the average size of the carbides is 0.5(m. This type of structure resembles a eutectic structure comprising of γ + carbides [10]. Solidification of this alloy commence with nucleation of austenite in the form of dendrites. During growth of these dendrites, excess carbon is rejected and accumulated between the dendrite, so the last liquid will solidify as eutectic. The extent of alloying seems to be improved when a higher power is used. Figure (4) showed more interdendritic regions in the sample processed at 4kW and 1500 mm/min. This means that more carbon is dissolve in this sample and consequently more interdendritic eutectic carbide is formed. EDS analysis was performed on these sample using the SEM microscope equipped with EDS analysis. Although carbon analysis is difficult due to the low power energy of the carbon peak, the EDS analysis gave carbon content about 2wt% in the sample shown in Figure (4b) and 3wt% in the sample shown in Figure (4b). This also has led to the dilution of the chromium and other alloying elements present in this steel.

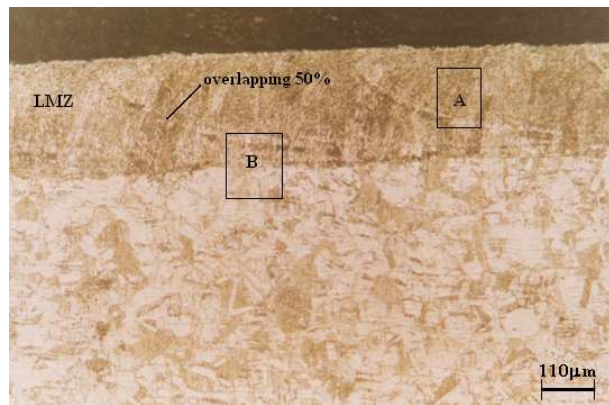


Figure 2: Optical micrographs shows cross section of the LMZ

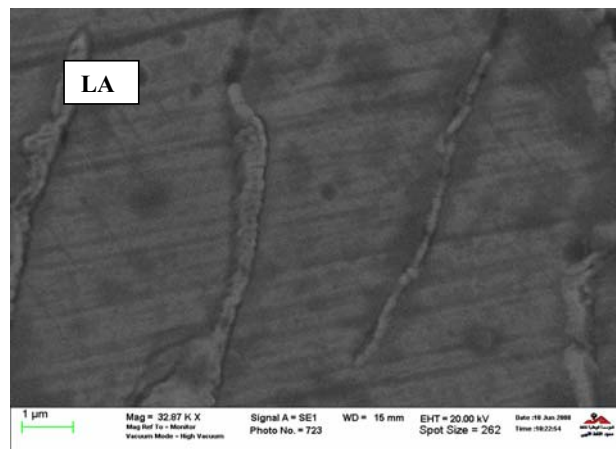
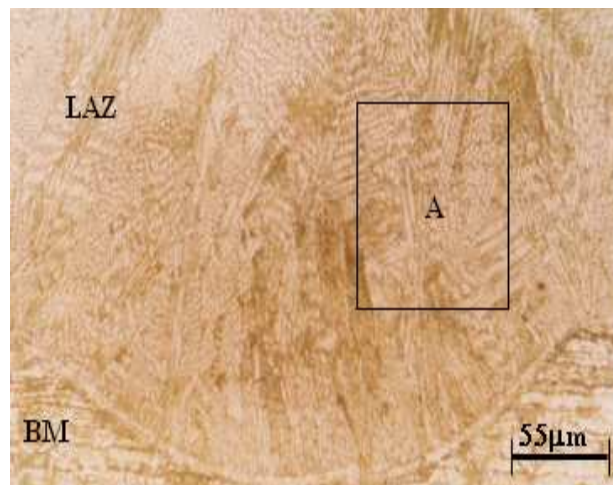


Figure 3: Optical micrographs show (a) cross section of the LAZ, (b) SEM of section A (2kW, 900 mm/min)

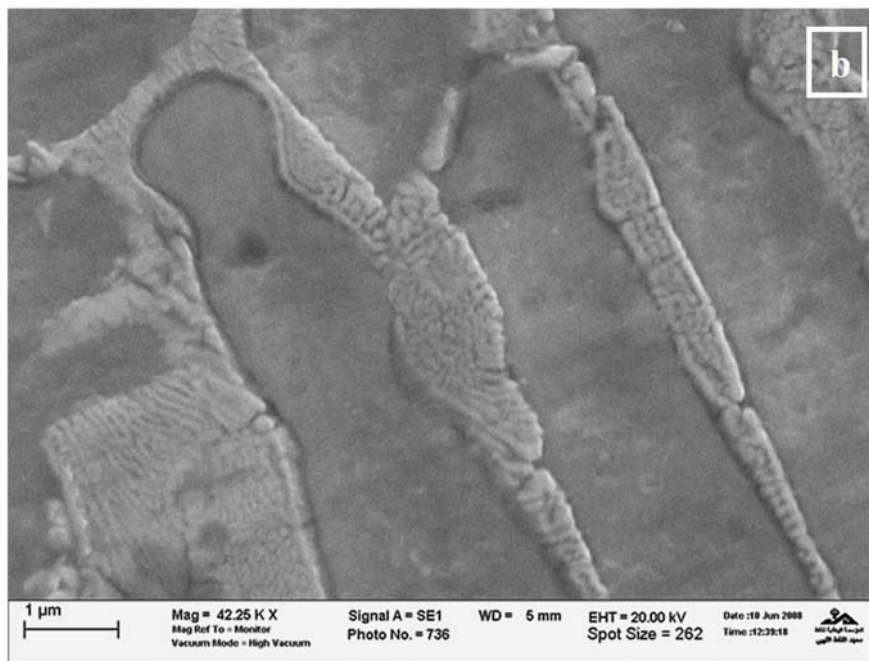
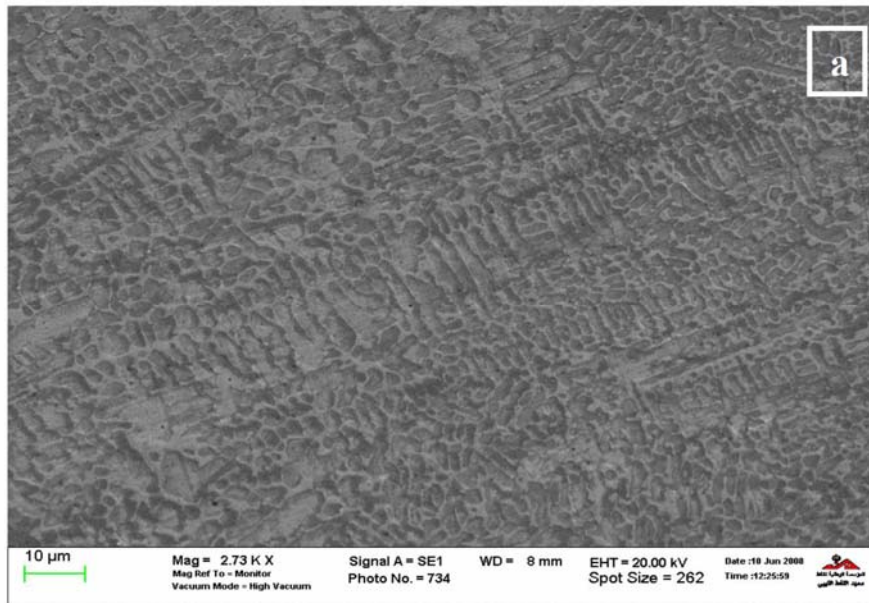


Figure 4: SEM micrographs show the LAZ produced at 4kW, (a) dendritic structure , (b) interdendritic structure at high magnification

X-ray diffraction

X-ray diffraction peaks from the surface of the un-treated, surface melted, and surface alloyed samples are shown in Figures (5a - c). It can be seen that the diffraction peaks from the surface of laser treated samples were similar to those of the untreated 316 steel, suggesting that the major phases has fcc structure. However, there is a shift in the position of peaks of the laser treated samples. This shift is not uniform. The degree of lattice expansion was different for each plane and was the largest for (200), suggesting no uniformity in the expansion of the cubic lattice. In the laser alloyed sample, a part from the fcc phase, there are other peaks identified as Cr_7C_3 . The increasing shift of the expanded austenite peaks in LSA sample presumably due to an increasing of carbon content in the austenite phase. The diffraction lines of the laser treated samples were slightly broadened compared with that of the untreated 316 steel. The observed line broadening is attributed to the presence of the stain and many defects such as dislocations in the surface layer due to high cooling rates and nonequilibrium solidification.

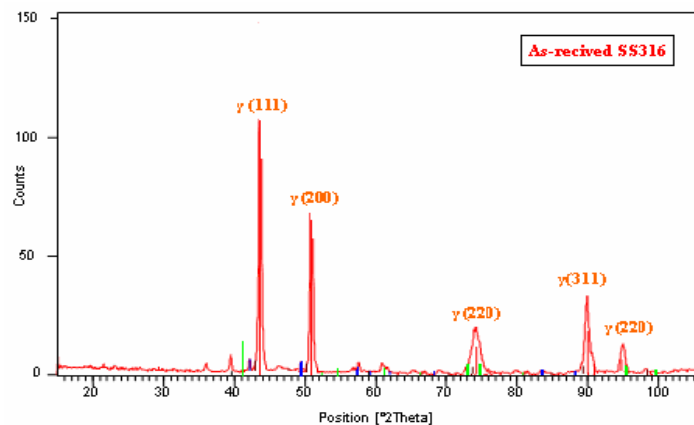


Figure 5 (a): X-ray diffraction patterns taken from the surface of (a) as received

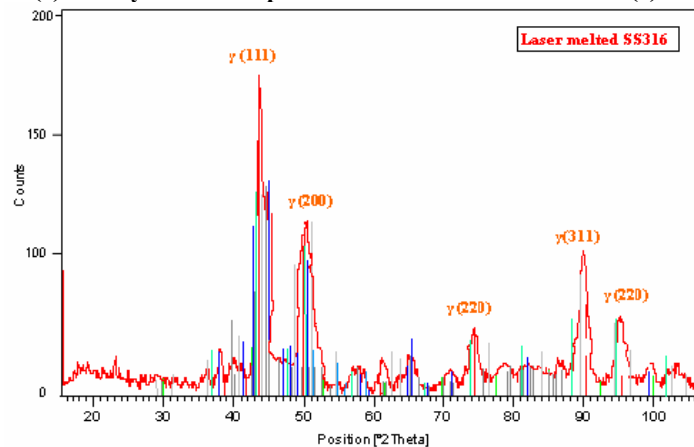


Figure 5(b): X-ray diffraction patterns taken from the surface of LMZ,

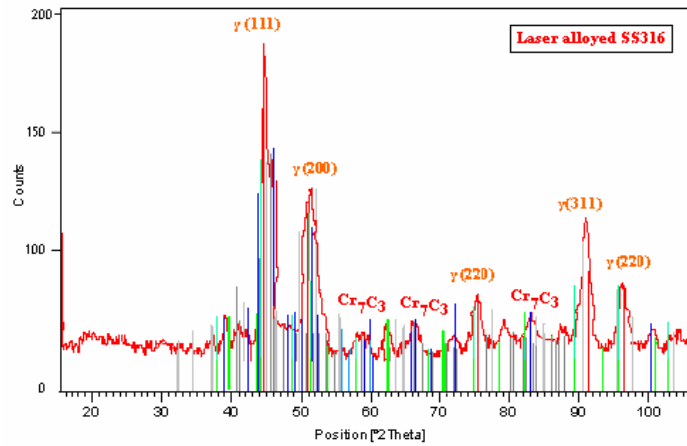


Figure 5 (c): X-ray diffraction patterns taken from the surface of LAZ (2kW and 1500 mm/min)

Microhardness

Microhardness profile across the melted and the alloyed zone is shown in Figure (6). The alloying with carbon increases the hardness specially at high power and also increases the depth to which the hardness extent. At 2kW, the maximum microhardness was ~ 470 extended to a distance ~ 200 μm below the surface followed by a sharp drop in hardness to a value of 200Hv. At 4kW, the maximum microhardness was ~ 500Hv extended uniformly to a depth of ~ 500 μm . These results can be interpreted by referring to Figure (4) which showed a high percentage of interdendritic regions resembling eutectic structure product consisting of austenite and carbides. The x-ray detects some extra peaks correspond to Cr_7C_3 which contribute to the hardening effect.

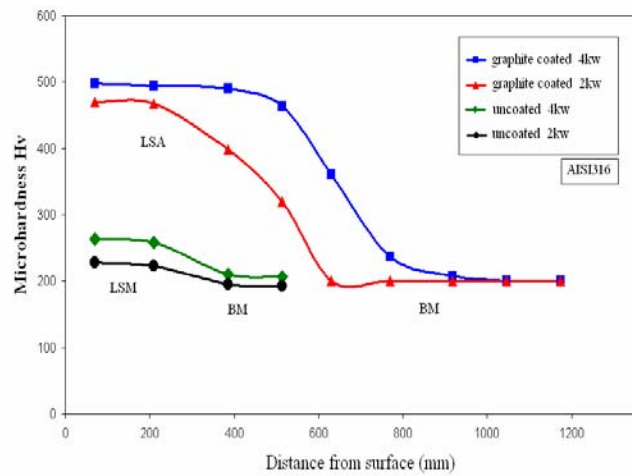


Figure 6: Microhardness profile across the melted and the alloyed zone depths produced at scanning speed 900 mm/min and different powers.

Corrosion behavior

Table (3) shows the corrosion current I_{Corr} and the corrosion rate C.R of the LSM and LAS samples processed at 2 and 4 kW laser power and 900 mm/min. It is apparent from the table that the C.R for the LSM sample is lower than the as received material at the two powers level used with more a decrease in the C.R at 4kW. However the situation is reversed when carbon is added to the laser melted zone by LSA technique. The C.R. of the samples alloyed with carbon is increased although this increase is low for the sample treated at 4kW. Also it can also be seen from Table (3) that the corrosion current increases and becomes higher after (LSA) which may indicate that the addition of the carbon to the 316 steel decrease the corrosion protection. The formation of carbide removes chromium from the surface and iron reducing its corrosion resistance. The improvement in corrosion resistant at laser power 4kW indicates that the processing parameters have a detrimental effect on the improvement of corrosion resistance.

Table 3: Corrosion parameter values for AISI 316 steel in 3.5% w/v sodium chloridesolution at ambient temperature after one hour and scanning speed.

Specimen No.	Surface condition	Power (kW)	I_{Corr} (mA/cm ²)	C. R (mm/year)
M*-14#	LSM	2	0.138	0.173
A*-20#	LSA	2	0.167	0.209
M-17#	LSM	4	0.133	0.166
A-23#	LSA	4	0.158	0.198
-	AISI 316	-	0.142	0.178

Figures (7 and 8) show polarization curves for 316 steel in 3.5% w/v sodium chloride solution at ambient temperature after one hour for LSM and LSA processed at 2kW and 4kW, respectively. It is clear that there was a shift in corrosion potential E_{corr} to more positive values in case of (LSM). This effect is due to the inhibiting effect of the self protective layer formed on the surface of the steel samples. It can be seen that the addition of the carbon (LSA) shifts the E_{corr} to more negative potentials and also increase the corrosion current value I_{corr}

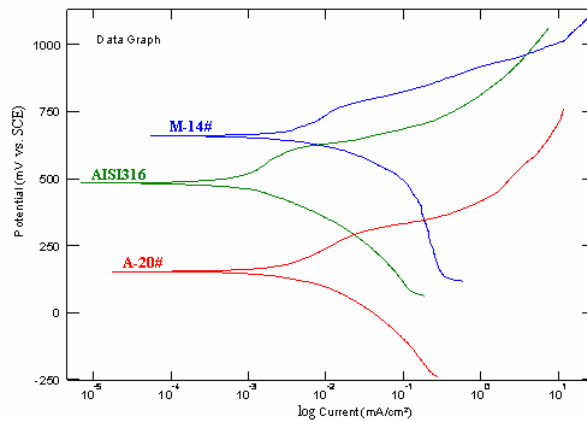


Figure 7: Polarizations curves for 316 steel in 3.5% w/v sodium chloride solution at ambient temperature after one hour and laser condition (2kW & 900mm/min)

It can be seen from this Figure (8) that 316 steel have the same behavior as in Figure (7) which is due that it has same corrosion mechanism in the both laser condition laser power 2kw and scanning speed 900 mm/min. Table (3) it can be seen that the addition of the carbon (LSA) shifts the E_{corr} . to more negative potentials and also increase the corrosion current value (I_{corr}) which confirm the suggestion of the formation of carbide removes chromium from the surface and iron reducing its ability to form a protective layer which reduce the corrosion.

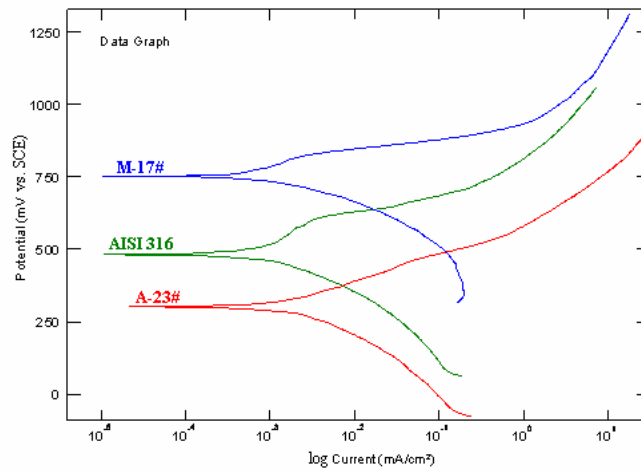


Figure 8: Polarizations curves for 316 steel in 3.5% w/v sodium chloride solution at ambient temperature after one hour and laser condition (4kW & 900mm/min)

CONCLUSIONS

Surface melting technique by laser irradiation is investigated as a process capable of producing surfaces with a unique microstructure and homogeneity and as a consequence to those, surface properties such as hardness and corrosion, might be improve. The following conclusions were obtained from this investigation

- Laser surface melting of 316 austenitic stainless steels using 2 and 4 kW allows obtaining a homogeneous modified surface layer with a very fine dendritic structure. The microhardness was not increased after melting treatment but corrosion resistant improved slightly especially when a high power is used. There was a shift in the I_{corr} toward a lower and more noble values after this treatment.
- Laser surface alloying by incorporating carbon into the laser melted zone produced a modified layer consisting of austenite dendrites surrounded with eutectic carbides. The solidified microstructure is dependent on the mixed carbon content. The microhardness increase significantly after laser alloying from 200 Hv to 500Hv. High hardness is associated with high carbon content.
- X-ray diffraction analysis showed that the high cooling rate associated with laser melting confirms did not affect the stability of the austenite. However extra peaks identified as Cr_7C_3 is detected coexisted with the austenite phase after laser alloying.
- The technique of laser alloying with carbon produces a hard surface but with a corrosion resistance inferior to that of the base metal.
- Surface melting improves the corrosion resistance while the surface alloying increases the corrosion rate. Better corrosion resistance is obtained when this steel is treated at high power.

- The change of electrochemical potential is more negative in the cast of LSA while it is more positive in the case of LSM which indicate an improvement in corrosion resistance.

ACKNOWLEDGMENTS

Acknowledgments are made to Husham Al-Mukherim in laser research center in Tripoli for his help in carrying out laser treatment and to the corrosion Lab in Gulf company, especially Eng. Aead Algderi and Mr. daoud Alabare for their permission to conduct the corrosion test.

REFERENCES

- [1] W.M.Steen: "Laser surface treatment of metals", (edited by C.W.Draper and P.Mozzoldi), NATO, ASI Ser, Vol.100 (1986) Kluwer Academic.
- [2] W.M.Steen, "Laser cladding, alloying, and melting", (ed. D.belforte and M Leritt), Tusla, OK, Penwell publishing company 1983.
- [3] J.D.Ayers, "Laser in metallurgy", (ed. Mukherjee and J.Mazumdar, Warrendale, PA, The metallurgical Society of AIME (1981)279.
- [4] B.L. Mordike, "Surface modification of metals", R.W. Cahn (Ed.), Materials Science and Technology. vol. 15. Processing of metals and alloys, VCH, Berlin. 1991. pp. 36.
- [5] Z Sun, I.Annergren, and, T.A.Mai, "Effect of laser surface remelting on the corrosion behavior of commercial pure titanium sheet", Material Sci. and Engg. A 345(2003) 293
- [6] O.M.A. Fakron and J.H.Abboud," Surface melting of nodular cast iron by Nd-YAG Laser and TIG", Journal of Materials Processing Technology 170 (2005) 127 -132
- [7] A.Walker, D.R.F.West, and W.M.Steen," Laser surface alloying of iron and 1C-1.4Cr steel with carbon", Metal Technology 11 (1984) 399-404.
- [8] J.H. Abboud, K.Y. Benyounis, A.G. Olabi and M.S.J. Hashmi, "Laser surface treatments of iron-based substrates for automotive application", Journal of Materials Processing Technology, 182 (2007) 427–431
- [9] A.I.Katsamas and G.N. Haidemenopoulos, "Laser – beam carburizing of low alloy steel", Surface and Coating Technology 139 (2001) 183-191.
- [10] A.Conde, R.Colaco, R.Vilar and J. Damborenea, "Corrosion behaviour of steels after laser surface melting", Materials and Design 21 (2000)441-445.
- [11] J.Damborenea C.F..Marsden, D.R.F.West, and A.J.Vazquez, "Pitting resistance of 420 stainless steel after laser melting treatment", Ninth European Congress on Corrosion, Utrecht, Holand, 1989, (1) paper FU-172.
- [12] C.T.Kwok, H.C.Man, and F.T.Cheng, "Cavitation erosion and pitting corrosion bahviour of laser surface melted martensitic stainless steel UNS S42000", Surface and Coating Technology 126 (2000) 238-255.
- [13] Ibrahim Y. Algathafi," Influence of laser surface melting of austenitic stainless steel on the microstructure and corrosion properties", M.Sc thesis, Department of Mechanical Engineering, University of Garyounis, Libya, 2008.